Entanglement of superconducting charge qubits by homodyne measurement

D A Rodrigues[1], C E A Jarvis[2], B L Györffy[2], T P Spiller[3] and J F Annett[2]

[1] School of Physics and Astronomy, University of Nottingham, Nottingham NG7 2RD, United Kingdom

[2] H H Wills Physics Laboratory, University of Bristol, Bristol BS8 1TL, United Kingdom

[3] Hewlett Packard Laboratories, Filton Road, Bristol, BS34 8QZ, United Kingdom

E-mail: [1] denzil.rodrigues@nottingham.ac.uk

E-mail: [2] catherine.jarvis@bristol.ac.uk

Abstract.

We present a scheme by which projective homodyne measurement of a microwave resonator can be used to generate entanglement between two superconducting charge qubits coupled to this resonator. The non-interacting qubits are initialised in a product of their ground states, the resonator is initialised in a coherent field state, and the state of the system is allowed to evolve under a rotating wave Hamiltonian. Making a homodyne measurement on the resonator at a given time projects the qubits into an state of the form $(|gg\rangle + e^{-i\phi}|ee\rangle)/\sqrt{2}$. This protocol can produce states with a fidelity as high as required, with a probability approaching 0.5. Although the system described is one that can be used to display revival in the qubit oscillations, we show that the entanglement procedure works at much shorter timescales.

1. Introduction

Central to the construction of any useful Quantum Information device will be an array of quantum systems whose collective quantum state can be prepared, measured or otherwise manipulated [1]. For the case of two-level systems—qubits—and in the solid state arena, small superconducting grains coupled to bulk superconductors via Josephson junctions, often referred to as Cooper-pair boxes, have been shown to be promising candidates for playing the role of the qubits[2]. Quantum state control has been demonstrated in single qubit devices through coherent or Rabi oscillations, observed with readout schemes consisting of either a single electron transistor (SET)[2] or quantronium[3] circuit coupled to the qubit being measured. Corresponding single qubit quantum state control results have also been obtained in superconducting flux qubit devices[4].

More recently, the coupling of such superconducting qubit devices has also been achieved[5, 6, 7]. Such coupling generates entangled two-qubit states, which is both of vital importance to possible quantum computing applications[1] , and also of interest in testing the fundamental limits of quantum mechanics in macroscopic objects[8, 9]. The two charge qubits of Pashkin *et al.*[5] were capacitively coupled, and each qubit independently measured with SET readouts. The resulting two-body density matrix, was consistent with the existence of non-classical correlations between the two qubits, although decoherence limited the fidelity of the CNOT gate which was attempted in the two qubit device[10]. Entanglement between superconducting flux qubit devices was reported by Berkley *et al.*[6]. A more recent experiment[7] showed antiphase oscillation of a two-qubit system, and detailed quantum state tomography established entanglement with 87% fidelity between two macroscopic superconducting charge-phase qubit devices[11]. Significant progress has also been made coupling superconducting charge[12, 13, 14] and flux[15] qubits to a quantum resonator mode, demonstrating effects such as the AC-Stark effect and resolving individual photon number states in the resonator. As well as being an essential part of any quantum computing protocol, the generation of entanglement is necessary for the demonstration of a Bells' inequality violation[16], which would prove unequivocally that the system cannot be described classically[17].

In all these experiments the coupling of the superconducting qubit to its measurement device has been shown to be one of the central aspects controlling its decoherence. Very long relaxation times were observed in the experiments of Wallraff *et al.*[12, 13, 14] in which the Cooper-pair box was coupled to a microwave stripline resonator, but not to any other measurement device. Measurement of a resonator dispersively coupled to a superconducting qubit has thus been shown to provide an excellent 'readout' system for the superconducting qubit[13, 18]. Quantum resonator modes therefore have real potential for both coupling and readout of superconducting qubits.

In this paper we present a measurement protocol by which entanglement may be

generated between two such superconducting qubits, which are coupled only though a common stripline resonator. We show that projective homodyne measurement on the resonator field may perform a projective measurement on the coupled qubit/field system, resulting in the generation of entangled states of the two qubits. It is interesting that there is assumed to be no direct coupling between the qubits themselves, and it is the act of projective measurement on the field which creates the entangled state. Our scheme for generation of entanglement is therefore analogous to the Knill, Laflame, Milburn or 'KLM' protocol[19] to generate entanglement of photons in linear quantum optics through projective measurement. In the same way, our scheme uses measurement to generate entanglement between qubits which have no other direct qubit-qubit interaction. The analysis presented here will be relevant for other physical systems consisting of two-level systems coupled via an harmonic mode such as atom-chips or nanomechanical systems.

Our work builds upon the extensive theoretical study of Meunier *et al.*[20] of collapse and revival phenomena of two level quantum systems coupled to a single quantized radiation mode. As is stressed by Meunier *et al.*[20] the rich variety of quantum phenomena displayed by the 'one qubit one mode' system is well known from Quantum Optics where the role of the two level system is played by a two level (Rydberg) atom[21]. A particularly striking example of these is the collapse and subsequent revival of the initial Rabi oscillations in the atom (qubit) section of the Hilbert space when the initial radiation field is in a coherent state $|\alpha\rangle$. Remarkably, as was first noticed by Gea-Banacloche [22], at times t, between the collapse time t_c and revival time t_r, when there are no Rabi oscillations, it is the radiation field part of the wave-function which manifests complex quantum behaviour. Following these insights we have studied the time evolution of the two qubit system coupled to a radiation mode. We show that simple projective homodyne measurements on the radiation field, at times between collapse and revival of multi qubit Rabi oscillations, may be used to obtain interesting entangled states of the two qubits.

The paper is structured as follows. In section 2 we introduce the two qubit version of the Jaynes-Cummings model[23, 24] and, in the interest of clarity, recall the current state of understanding of the complex evolution with time of a combined qubit and field state. We also discuss the expected results of a homodyne measurement on the field variable of our system. The main results of this paper are developed in section 3 where we describe and analyse a simple experimental protocol which involves homodyne measurements on the field variable and results in heralded maximally entangled states of the qubits. Our general conclusions are presented in section 4.

2. Jaynes-Cummings model for two qubits coupled to a resonator

The salient features of one qubit coupled to a single mode of the radiation field can be described approximately by the Jaynes-Cummings model[23], much studied in quantum optics. This model has generated a great deal of interest in the past as it exhibits

interesting behaviour[21] and it has been used to describe quantum correlation.

In this paper we consider two charge qubits each coupled capacitively to a stripline resonator using the two qubit Jaynes-Cummings model[24]. If the qubits are placed at an antinode of the fundamental harmonic mode of the resonator, then we can describe the system as a pair of two-level systems coupled to a simple harmonic oscillator. The charging energy of the qubits and their coupling to the resonator can be controlled by the application of magnetic and electric fields[2]. If these are tuned so that the qubits are close to resonance with the field we can describe the system using a rotating wave Hamiltonian,

$$\hat{H} = \hbar\omega\left(\hat{a}^\dagger\hat{a} + \frac{1}{2}\right) + (E_1\hat{\sigma}_1^z + E_2\hat{\sigma}_2^z) + \hbar\sum_{i=1}^{2}\lambda_i\left(\hat{a}\hat{\sigma}_i^+ + \hat{a}^\dagger\hat{\sigma}_i^-\right) \tag{1}$$

where

$$\hat{\sigma}^z = |e\rangle\langle e| - |g\rangle\langle g|,\ \hat{\sigma}^+ = |e\rangle\langle g|,\ \hat{\sigma}^- = |g\rangle\langle e|, \tag{2}$$

$\hat{a}^\dagger$ and $\hat{a}$ are the creation and annihilation operators of photons with frequency ω, $E_{1,2}$ are the charging energies of the qubits, and $\lambda_{1,2}$ the resonator-qubit coupling terms. We consider the system to be exactly on resonance, for simplicity, and also assume that the Cooper pair boxes have equal charging energy, ($E_{1,2} = E$) and coupling to the resonator, ($\lambda_{1,2} = \lambda$). In the rotating wave approximation, we notice that states with m excited qubits and n photons only couple to states with $m' + n' = m + n$. This means that we can describe the system as an infinite set of non-interacting four level sub-systems all labeled by $n + m$. We can find the solution of each of these sub-systems analytically, and then sum over these to obtain the state of the whole system.

For an initial state,

$$|\psi(t)\rangle = |gg\rangle\sum_{n=0}^{\infty}C_n|n\rangle \tag{3}$$

we obtain,

$$\begin{aligned}|\psi(t)\rangle = \sum_{n=0}^{\infty}&\exp\left(-i\frac{\omega}{2}(2n-1)t\right)C_n\\ &\left[\frac{\sqrt{n(n-1)}}{2n-1}\left(\cos\left(\lambda t\sqrt{2(2n-1)}\right)-1\right)|ee,n-2\rangle\right.\\ &- i\frac{\sqrt{n}}{\sqrt{2(2n-1)}}\sin\left(\lambda t\sqrt{2(2n-1)}\right)(|eg,n-1\rangle + |ge,n-1\rangle)\\ &\left.+\frac{1}{2n-1}\left(n\cos\left(\lambda t\sqrt{2(2n-1)}\right)+(n-1)\right)|gg,n\rangle\right]\end{aligned} \tag{4}$$

where the state $|eg,n\rangle$ is the tensor product of a Fock state $|n\rangle$ of the photons and the state of the qubits which is either excited (e) or ground (g) for each qubit. For brevity

we only discuss the solution for the case where the qubits both start in their ground state, but we note that the solution with a general initial condition is generically similar. The initial state of the field is determined by the coefficients C_n, which for a coherent state $|\alpha\rangle$ are given by,

$$C_n = e^{-|\alpha|^2/2}\frac{\alpha^n}{\sqrt{n!}}, \tag{5}$$

with the phase, θ, and average occupation, $\bar{n}$, of the coherent state determined by $\alpha = \sqrt{\bar{n}}e^{-i\theta}$.

In spite of its relative simplicity equation (4) describes a wide range of interesting phenomena. A much studied example of these is the collapse and revival of Rabi oscillations. In this paper we shall be concerned with phenomena at times where there are no Rabi oscillations. To illustrate the generic behaviour of $|\psi(t)\rangle$ in equation (4) we shall now comment on the qubit and the photon sector separately. If we consider the state of the qubits after tracing out the field state, the probability of the qubits being in the state $|gg\rangle$ is,

$$P_{gg}(t) = \langle gg|\rho^Q(t)|gg\rangle = \sum_{n=0}^{\infty} |\langle gg, n|\psi(t)\rangle|^2 \tag{6}$$

where $\rho^Q(t)$ is the reduced density matrix at a certain time for the qubits when the field has been traced out. In agreement with Iqbal *et al.*[25], we find the results depicted in figure 1. Evidently we see that initial oscillations of the qubit states decay rapidly, after which the qubit is in a mixed state. After a period of time, the oscillations revive, indicating the information about the qubits' initial state has returned to the qubits from the field. We see a larger revival at the revival time, $t_r = 2\pi\sqrt{\bar{n}}/\lambda$, which is proceeded by a smaller revival at $t_r/2$. The smaller revival is not seen for the one qubit case and this is due to the extra frequency introduced by the addition of the second qubit.

So far we have studied the time evolution of the reduced density matrix of the qubits. To investigate the radiation field it is useful to calculate the Q function [26],

$$Q(\alpha, t) = \langle\alpha|\rho^F(t)|\alpha\rangle \tag{7}$$

where $\rho^F(t)$ is the reduced density matrix at a certain time for the radiation field when the qubits have been traced out. The values of $Q(\alpha, t)$ in the complex alpha plane at fixed times are shown in figure 2.

The Q function shows a set of three 'blobs', each representing a mesoscopic wavepacket of the cavity field. As a function of time the three wavepackets move around the complex plane and follow the circular path of radius $\sqrt{\bar{n}}$. Although the wavepackets all begin in the same place, they evolve with different frequencies, so the states begin to separate. After a period of time, depending on the differences between the frequencies, the different sub-distributions are separated by more than their diameter and can be easily distinguished, (figure 2b).

To elucidate the connection between the collapse and revival in the qubit part of the Hilbert space and the peaks in the $Q(\alpha, t)$ distribution depicted in figure 2 we recall

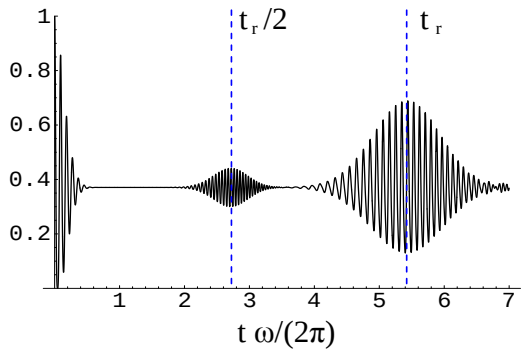

Figure 1. Revival of the initial state of the qubit system. The curve shows the probability that the qubits are in the state $|gg\rangle$ after tracing out the resonator. The initial qubit oscillations rapidly decay, indicating the qubits are in a mixed state. The revival of the oscillations indicates that the information about the qubit states has been transferred back to the qubits from the resonator. The main revival occurs at $t_r = 2\pi\sqrt{\bar{n}}/\lambda$, with a partial revival at $t_r/2$. We have chosen $\omega = \lambda = 1$ and $\bar{n} = 30$.

briefly the results of Meunier *et al.*[20] obtained in the large $\bar{n}$ limit. Generalising the one qubit result of Gea-Banacloche for the two qubit case they found that $|\psi(t)\rangle$ can be written as a superposition of Gea-Banacloche states described below.

$$|\psi(t)\rangle = \sum_{k=-1}^{1} |D_k(t)\rangle \otimes |\Phi_k(t)\rangle \tag{8}$$

where k=-1, 0, or 1, $|D_k(t)\rangle$ is a state of the qubits and $|\Phi_k(t)\rangle$ is the state of the field.

$$|D_{-1}(t)\rangle = \frac{1}{4}(e^{-2i(\omega-\frac{\lambda}{\sqrt{\bar{n}}})t}e^{-2i\theta}|ee\rangle - e^{-i(\omega-\frac{\lambda}{\sqrt{\bar{n}}})t}e^{-i\theta}(|eg\rangle + |ge\rangle) + |gg\rangle) \tag{9}$$

$$|D\ _0(t)\rangle = \frac{1}{2}(|gg\rangle + e^{-2i(\theta+\pi/2+\omega t)}|ee\rangle) \tag{10}$$

$$|D\ _1(t)\rangle = \frac{1}{4}(e^{-2i(\omega+\frac{\lambda}{\sqrt{\bar{n}}})t}e^{-2i\theta}|ee\rangle + e^{-i(\omega+\frac{\lambda}{\sqrt{\bar{n}}})t}e^{-i\theta}(|eg\rangle + |ge\rangle) + |gg\rangle) \tag{11}$$

$$|\Phi_k(t)\rangle = e^{-ik\lambda\sqrt{\bar{n}}t}|e^{-i(\omega+k\frac{\lambda}{\sqrt{\bar{n}}})t}\alpha\rangle \tag{12}$$

The state of the field in each Gea-Banacloche state $|D_k(t)\rangle \otimes |\Phi_k(t)\rangle$ is one of three coherent field states $|\Phi_k(t)\rangle$, each of which has a phase that evolves with a frequency given by $\omega + k\frac{\lambda}{\sqrt{\bar{n}}}$. Each field state corresponds to a particular qubit state $|D_k(t)\rangle$, as given by equations (9)-(11). In particular, we note that qubit state $|D\ _0\rangle$ corresponding to the field state $|\Phi_0(t)\rangle$ is a superposition of $|gg\rangle$ and $|ee\rangle$ only, and has no components of the states $|ge\rangle$ or $|eg\rangle$, a fact that we shall exploit to produce our entanglement protocol.

The Gea-Banacloche states can be clearly seen in figure 2, where the three 'blobs' represent the states $|\Phi_k(t)\rangle$, and we see that the frequency at which these

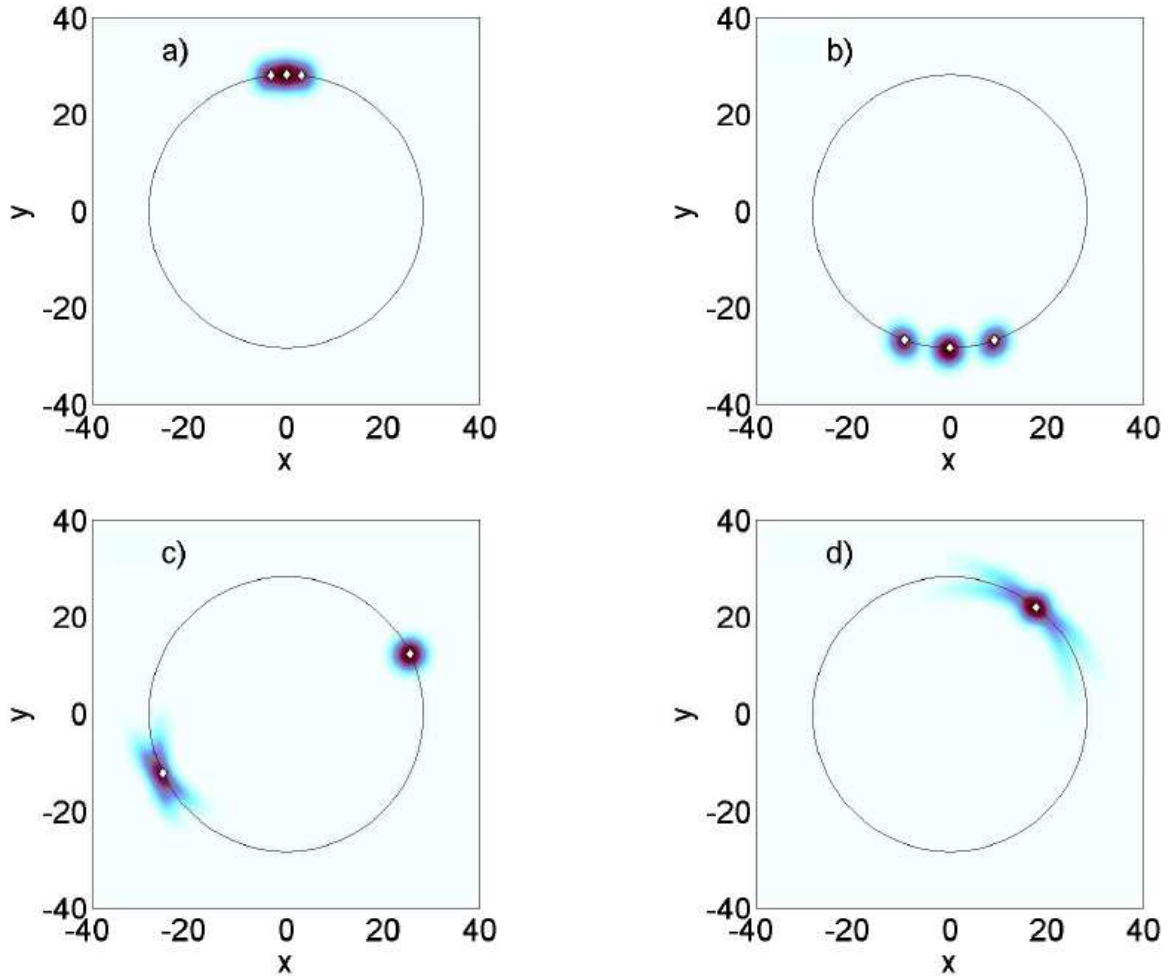

Figure 2. Phase-space plots of the Q-function for four different times, where the dimensionless $x = \alpha + \alpha^*$ represents the electric field and $y = (\alpha - \alpha^*)/i$ represents the magnetic field. Also plotted are white diamonds corresponding to the evolution of the field states in equation (12). (a) $t = \pi/(2\omega)$: The phase space close to $t = 0$, when the peaks are not well separated, (b) $t = 3\pi/(2\omega)$: After a period of time the sub-distributions, evolving with different frequencies, separate and can easily be distinguished, (c) $t = t_r/2$: The time at which there is the first occurrence of spontaneous revival, (d) $t = t_r$: Location of the states at the second main revival peak. For all the diagrams $\lambda = \omega = 1$ and $\bar{n} = 200$.

sub-distributions move around the complex plane is determined by the frequencies in equation (12). The well known collapse and revival phenomena, seen in figure 1, can now be understood in terms of the evolution of the Gea-Banacloche states. The Rabi oscillations collapse when the field states are well separated (figure 2(b)). At the large revival peak (figure 2(d)) all the distributions overlap in the complex plane, which occurs when all the field states are in phase. The time this occurs is determined by the condition $\exp(i\omega t) = \exp(i(\omega + \lambda/\sqrt{\bar{n}})t) = \exp(i(\omega - \lambda/\sqrt{\bar{n}})t)$. This condition is fulfilled by $t_r = 2\pi\sqrt{\bar{n}}/\lambda$. At an earlier time we observe a smaller revival peak, when two of the states are in phase (figure 2(c)). This occurs when

$\exp(i(\omega + \lambda/\sqrt{\bar{n}})t) = \exp(i(\omega - \lambda/\sqrt{\bar{n}})t)$, namely at $t = t_r/2$.

After gaining a clearer understanding of the physics by taking the large-$\bar{n}$ limit, we now return to our exact calculations based on equation (4). Whilst the Q-function shows a fuller understanding of the state at a specific time, we shall study an experimentally more accessible distribution defined as follows. Evidently the eigenvalues of the operator $\hat{x} = (a + a^\dagger)$ are related to the position variable (electric field) of the harmonic oscillator which describes the cavity mode. In order to analyze the behaviour of this system as a function of time, we can plot the corresponding x-distribution of the field state after we have projected out the qubit states, i.e. we plot

$$P_r(x,t) = \langle x, r|\rho(t)|x, r\rangle \tag{13}$$

where $r = gg, ee, eg, ge$ (figures 3(a) - 3(d)). A convenient numerical method for obtaining this distribution is to project out a particular qubit state, transform the density matrix into the x-basis and take the diagonal elements. Obviously, the finite number of basis states in the calculation will lead to a discrete set of position eigenvalues x_i for $\hat{x}$, and hence a discrete set of probabilities $P_r(x_i, t)$, but this set of points can be made sufficiently dense to form a probability density, as given in equation (13).

Although the $Q(\alpha, t)$ function studied by Meunier *et al.* [20] gives a fuller account of the cavity field than the above $P_r(x_i, t)$, nevertheless, as shown in figure 3, the latter also captures the salient features of a very interesting quantum state at hand. In the interest of clarity the pictures in figure 3 are at the same times as the pictures in figure 2.

As in figures 2(a) - 2(d) we can see that although the distributions initially overlap, they evolve with different frequencies, so the peaks begin to separate (figure 3(b)). After a period of time the distributions overlap and cause the two revival peaks (figures 3(c) and 3(d))

3. Entanglement protocol

The basis behind the proposed entanglement procedure is a measurement of the quantum field at some chosen time, which projects the state of the two qubits into an interesting and useful entangled state, heralded by the outcome of the field measurement. In quantum optics the idea of measuring one part of an entangled system to learn something about the other goes back over twenty years [27, 28]. Measurement of a coherent state entangled with a photon can be used to project the photon state without absorption of the photon. In our case there is a tripartite entangled system and projective measurement of the coherent state is used to project the remaining bipartite qubit system. The relevant measurement is balanced homodyne detection, where the coherent state is mixed with a strong local oscillator field on a 50:50 beam-splitter before photo-detection of the two outgoing fields. It is well known, e.g. [29], that in the strong local oscillator limit the photon counting measurements made on the two outgoing modes of the beam-splitter correspond to a projector (e.g. $|x\rangle\langle x|$) onto a chosen

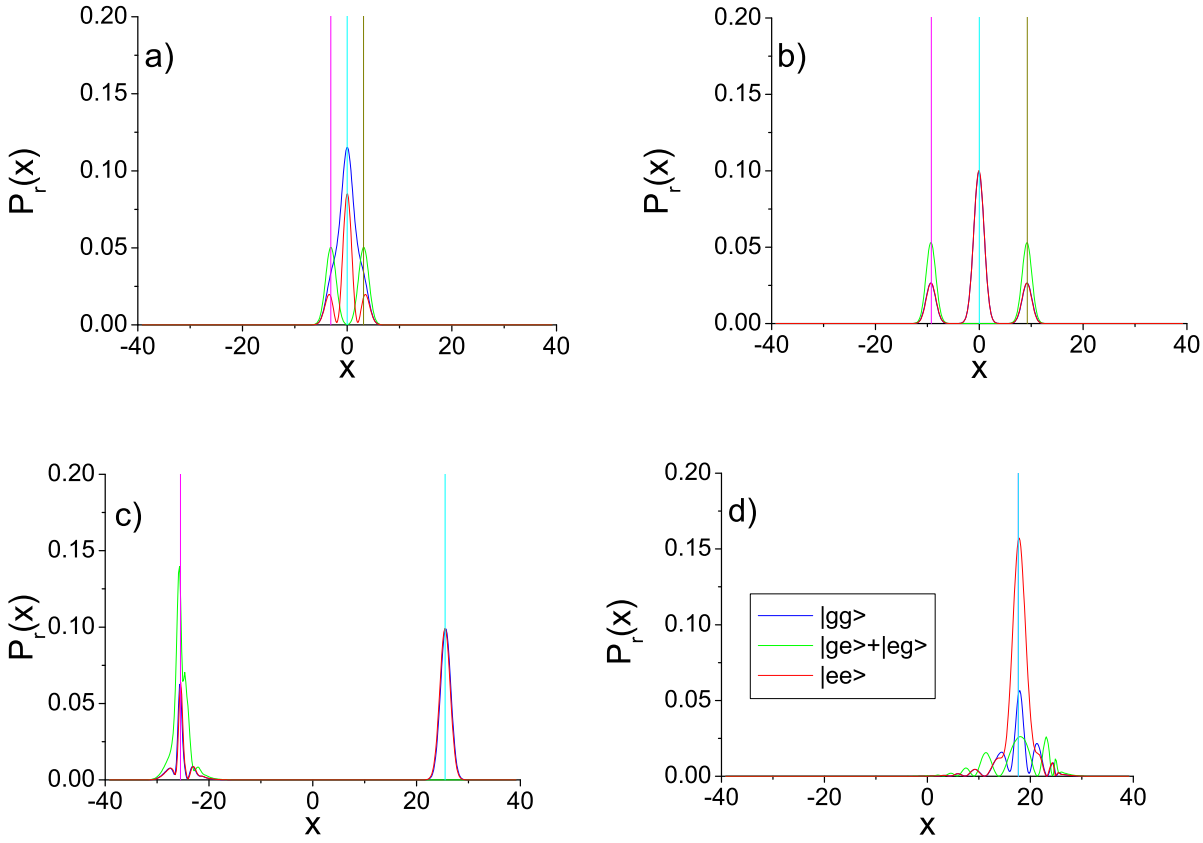

Figure 3. The x-quadrature distribution of the field state after projecting out the qubits states $r = |gg\rangle, |ee\rangle, |ge\rangle + |eg\rangle/\sqrt{2}$ for a series of different times. The vertical lines indicate the location of the field states as given in equation (12). (a) $t = \pi/(2\omega)$: The x-distribution close to $t = 0$, when the peaks are not well separated, (b) $t = 3\pi/(2\omega)$: After a period of time the sub-distributions, evolving with different frequencies, separate and can easily be distinguished, (c) $t = t_r/2$: The x-distribution at the first revival peak, (d) $t = t_r$: The x-distribution at the second main revival peak. The vertical lines indicate $x(t)$ for harmonic oscillators with frequencies $\omega, \omega \pm \lambda/\sqrt{\bar{n}}$. For all the diagrams $\lambda = \omega = 1$ and $\bar{n} = 200$.

quadrature of the initial coherent state field being measured, where the quadrature is set by the chosen phase of the local oscillator field. As will be seen for our system, at certain times a projection onto the x quadrature of the field entangled with the qubits can leave the qubits in an entangled state. For the case of superconducting qubits coupled to a microwave field mode [30, 31] this requires homodyne detection at microwave frequencies, rather than the familiar beam-splitter and photo-detection systems employed at optical frequencies. The mixing (of signal and local oscillator) and detection at microwave frequencies, in order to project onto a defined quadrature of a microwave coherent state field, may be achievable through use of a single electron transistor (SET), as has been discussed in detail in [32].

We stress that in our entanglement protocol, the idea is to introduce, or turn on, the homodyne measurement applied to the cavity field at some chosen time. This would require some sort of fast (on the time-scale of the qubit/field evolution discussed in the previous section) opening or gating of the cavity, to enable the microwave field to be subject to measurement at a chosen time. Given the long coherence times (or, correspondingly, high quality factors) observed in superconducting qubit and microwave mode experiments [12, 13, 14], we neglect decoherence in the field mode and qubits prior to the measurement, but explicitly allow for the decoherence of the actual measurement process, through its projection of the state of the qubits and field.

So, taking homodyne measurement to act as a projective measurement of x, our entanglement procedure is as follows. At a given time t the x-quadrature measurement will give a value of x taken from the distribution $P(x,t) = \sum_r P_r(x,t)$. Repeated observations would measure the whole distribution $P(x,t)$. Now if the peaks in $P_r(x,t)$ are well separated for different qubit states r, then the result of a single x-measurement indicates which sub-distribution $P_r(x,t)$ the system is in, and thus the value of r for that single measurement. Hence the qubit state r is *conditioned* on the result of the measurement of x. If this state is an entangled one then we have created an entangled state out of the unentangled initial condition $|gg\rangle$ by making the measurement. Furthermore, the creation of the entangled state, although probabilistic, is heralded on the result of the x-measurement, i.e. the result of the measurement tells us which peak of the distribution we are in, and hence whether or not we were successful in our attempt to create the state. Equations (8)-(12) show that if the measurement result corresponds to the field state $|\Phi_0(t)\rangle$, the qubit state will be a superposition of the states $|gg\rangle$ and $|ee\rangle$, with a relative phase given by $\phi = 2(\theta+\pi/2+\omega t)$. Although this state is maximally entangled for any given phase, a two-qubit state with unknown phase has no extractable entanglement and can be regarded as mixed. Thus we specify a particular *target state* with a chosen phase and try to produce this given state.

We would like to know how efficient this protocol is at producing a given target state. We can ask this question in the following way: if a projective measurement is made on x, what is the probability that the state of the qubits after the measurement will have a fidelity (given by $F = |\langle a|b\rangle|^2$ for two pure states $|a\rangle$ and $|b\rangle$) greater than F_{min} with our target state? We call this value the probability of success, P_s.

$$P_s(t) = \sum_i P(x_i,t)\Theta(F - F_{min}) \tag{14}$$

where $\Theta(F - F_{min})$ is zero for $F \leq F_{min}$ and unity for $F > F_{min}$. This criterion both allows us to specify *how good* our state is and tells us *how often* the procedure works. In figures 4 and 5 P_s is plotted for the maximally entangled state $(|ee\rangle + |gg\rangle)/\sqrt{2}$ as a function of time, with a minimum fidelity $F_{min} = 0.9$.

We find that P_s shows a series of flat-topped peaks as a function of time, figure 4, occurring at twice the resonator frequency ω, indicating that the there is a significant chance that the measurement will produce the state $(|ee\rangle + |gg\rangle)/\sqrt{2}$ twice every

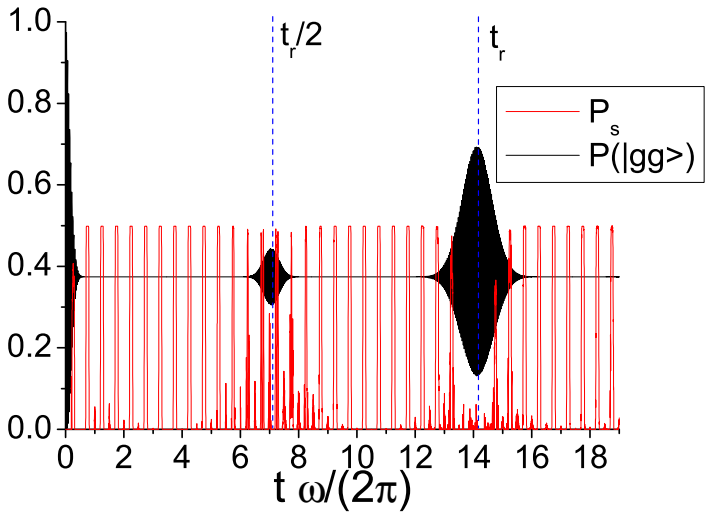

Figure 4. Revival of the qubits' initial state and the probability the entanglement procedure is successful, P_s. The black curve shows the probability that the qubits are in the state $|gg\rangle$, tracing over the resonator. The (lighter) red curve shows the probability of obtaining the state $(|gg\rangle + |ee\rangle)/\sqrt{2}$ with a fidelity $F \geq F_{min}$, P_s, as a function of time. The vertical dashed lines indicate the revival and sub-revival times at $t_r = 2\pi\sqrt{\bar{n}}/\lambda$ and $t_r/2$ respectively. We have chosen $\lambda = \omega = 1$, $\bar{n} = 200$ and a minimum fidelity $F_{min} = 0.9$.

oscillation cycle. Note that the probability of producing this state is quite large (close to 0.5) for a significant period of time. We obtain the state $(|ee\rangle + |gg\rangle)/\sqrt{2}$ when the measurement of x corresponds to the peak with frequency ω (the central peak in figure 3b). The peaks are most widely separated at the time $t_r/4$, but it is worth emphasising that we observe peaks in P_s close to 0.5 as soon as the peaks do not overlap, i.e. at a much shorter time than the revival.

At other points in the oscillation cycle, the qubits will have a different relative phase. In figure 5 we have also plotted the probability of obtaining the states $(|ee\rangle + e^{-i\phi}|gg\rangle)/\sqrt{2}$ with $\phi = 0, \pi, \pm\pi/2$. We can therefore produce any of the maximally entangled states of the form $(|gg\rangle + e^{-i\phi}|ee\rangle)/\sqrt{2}$ by making the projective measurement at the appropriate time.

We might expect that as the phase is evolving continuously, we would only get the desired target state at instantaneous points in time. The fact that we can still get a non-zero P_s for a finite time is due to two factors: firstly that the states $(|gg\rangle + e^{-i\phi}|ee\rangle)/\sqrt{2}$ for different ϕ's are not orthogonal, and secondly that the coherent state has a finite size.

States with different values of ϕ are not in general orthogonal. Of course, if we were to require that we obtain our target state with unit fidelity, then we would expect to obtain our target state only at a single moment in time, and indeed the peaks in P_s get narrower as F_{min} is increased. However, if we choose an $F_{min} < 1$ which we consider

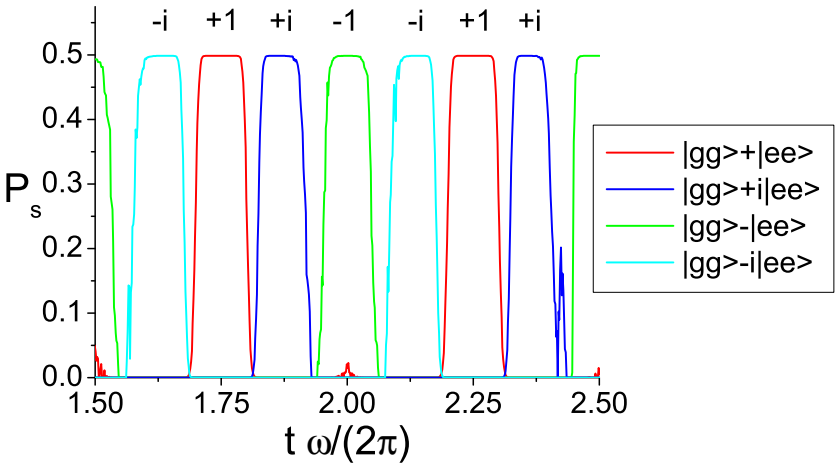

Figure 5. The probability, P_s, of achieving a fidelity greater than 0.9 for target states of the form $(|gg\rangle + e^{i\phi}|ee\rangle)/\sqrt{2}$ with phases $0, \pi, \pm\pi/2$. The coupling is given by $\lambda = \omega = 1$, and $\bar{n} = 200$. The curves all reach a constant value close to 0.5 for a finite period. The value of $\exp(i\phi) = \pm 1, \pm i$ for the state produced is indicated above each peak.

"good enough," then a range of values of ϕ will have fidelity greater than this with the target state. This leads to a simple trigonometric relationship between the width of the peak in P_s and the desired fidelity,

$$\Delta t^{\infty} = \frac{\arccos(2F_{min} - 1)}{\omega}, \tag{15}$$

which is shown in figure 6. In the limit $\bar{n} \to \infty$, we find that P_s as a function of time is a

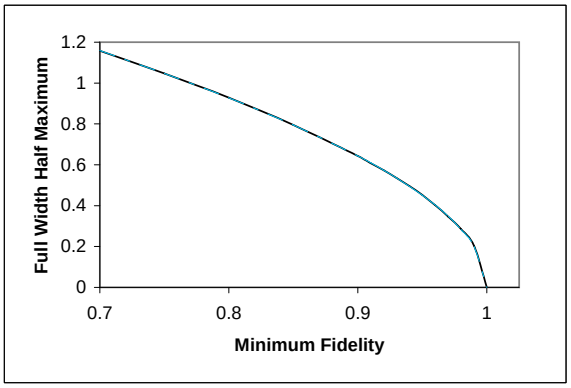

Figure 6. Full width at half maximum height for the P_s peak, as a function of fidelity. The numerically calculated value for $\bar{n} = 300$ (light blue dashed line) is compared to the analytical form in equation (15) (black line). We get good agreement between these even for values of $\bar{n}$ where the peak shows significant broadening because the shape of the peak (figure 7) changes in such a manner that the FWHM value is relatively unaffected.

series of top-hat functions with a width given by equation (15) and a height of 0.5. The

projective measurement "perfectly" produces a state of the form $(|gg\rangle + e^{-i\phi}|ee\rangle)/\sqrt{2}$ and the width of the peaks in P_s is solely due to the finite overlap between this state and the target state.

For finite $\bar{n}$ coherent states we see in figure 7 that the value of P_s changes continuously, rather than as a top-hat function. This smoothing is due to the fact that the coherent state has a finite width. If the centre of the peak in the x-distribution corresponds to the state $(|gg\rangle + e^{-i\phi}|ee\rangle)/\sqrt{2}$ the leading and trailing edges of the peak correspond to qubit states with phases slightly above or below ϕ. This means that even when the centre of the peak has a fidelity lower than F_{min}, the leading or trailing edge may have the target value of ϕ, leading to peaks in P_s with a greater width, as can be seen in figure 7. The difference in phase across the distribution also means that when the centre of the peak has the desired phase, the edges of the peak have the "wrong" phase and P_s will be reduced (observable as a reduction of the step height in figure 7). As $\bar{n}$ is increased, the difference in phase between the edges and centre of the peaks disappears, so that for $\bar{n} \to \infty$, the whole of the peak corresponds to the exact state. Numerical calculations indicate that the width of the peak is approximately given by the "ideal" width Δt^{∞}, plus a term due to the finite size of the coherent state,

$$\Delta t_{FWQM} = \frac{K(F_{min})}{\sqrt{\bar{n}}} + \Delta t^{\infty} \tag{16}$$

where $K(F_{min})$ is a constant that depends on F_{min}.

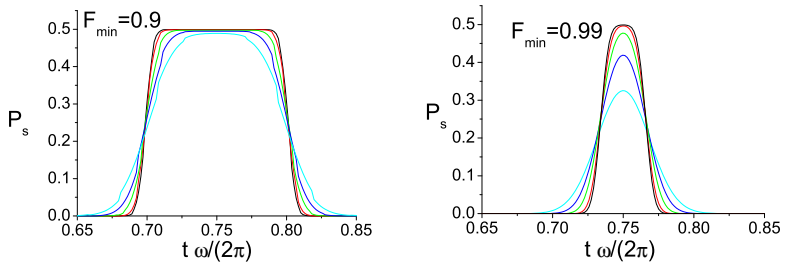

Figure 7. The probability, P_s of achieving desired fidelity F_{min} as a function of time over one peak, plotted for coherent states with $\bar{n} = 300, 200, 100, 50, 25$ (top to bottom). The two sub-plots show P_s for different values of F_{min}. For large coherent states and low F_{min} the peaks approach a top-hat form. For smaller coherent states or larger F_{min} the states become more rounded.

There are some points in the evolution that do not lead to a high value of P_s for any phase ϕ. This can be observed in figure 5, where the peaks in P_s for the states with phases $\phi = 0, \pm\pi/2$ overlap (indicating a continuous change from one state to the other), but P_s is zero for a finite period between the peaks representing states with $\phi = \pi$ and $\phi = \pm\pi/2$. These periods, which occur four times a cycle, represent the times when two of the x-distribution peaks overlap and so the qubit state produced by the x-measurement is not of the form $(|gg\rangle + e^{-i\phi}|ee\rangle)/\sqrt{2}$.

In the limit of $\bar{n} \to \infty$, the peaks in P_s are step functions of height 0.5 with a width determined by equation (15), which means we can achieve any desired fidelity with a probability of close to 0.5 as long as we can measure x at an exact time. Of course, we do not have instantaneous measurements, and so, depending on the desired fidelity and the time resolution of the measurement, it may be desirable to have a smaller coherent state. As F_{min} increases, we see that the width of the step function decreases (figure 6), meaning that the measurement must occur within an increasingly specific window in time. If this becomes a limiting factor, it may be preferable to use a smaller coherent state, increasing the window in which a high fidelity state can be found at the expense of reducing the probability of obtaining that state. An additional problem in any real measurement will be imprecise in space as well as time, i.e. the value of x returned by the measurement is probabilistic. It is clear that if the imprecision in the measurement is much smaller than the widths of the peaks in the x-distribution, then the imprecision will have little effect, and we can treat the measurement as projective. However, we also find that as long as the imprecision is smaller than the separation between peaks, the protocol still produces high fidelity states, although the effect of finite $\bar{n}$ in reducing the fidelity becomes more pronounced.

It should also be noted that this technique can easily be scaled up to entangle larger numbers of qubits. For larger numbers of qubits the entanglement of the states created is not as easy to quantify, and it may not be possible to couple them to the resonator with equal strength, and so further research is required in this area.

4. Conclusions

We have described a system of two qubits capacitively coupled to a superconducting microwave resonator, and shown that we can devise a protocol for heralded probabilistic production of entangled states of the qubits. This method only requires an initial preparation of the system in a product state of the qubit ground states, a coherent state of the field in the resonator, and the ability to perform a homodyne measurement on the resonator. This protocol can produce states with a fidelity as high as desired with a probability approaching 0.5 in the limit of an infinitely large coherent state. We have shown that there is a trade-off between the fidelity desired, the probability of obtaining the desired state and the time window in which the measurement must be performed. Choosing a smaller coherent state increases the time window of measurement but reduces the probability of obtaining the desired fidelity.

We have shown that this protocol is in some sense the dual of the phenomenon of revival in that both cases rely on the fact that we can regard the whole system as consisting of several field coherent states for each qubit state, with the different field states oscillating with different frequencies. Revival occurs when the time evolution of these states at these frequencies brings them all into phase with each other. In contrast the entanglement protocol works best when the states are well separated in phase.

Being based on measurement of a quantum mode, which is coupled separately to

both qubits, our approach to generating entanglement contrasts with approaches where the two qubits, although not interacting directly with each other, are both coupled directly to the same measurement apparatus or detector. A solid state qubit example of this is given by Ruskov and Korotkov [33], for two quantum dots coupled to a point contact, or two Cooper-pair boxes coupled to a SET. Our entangling protocol also contrasts with approaches such as that of Schneider and Milburn[34], where the common resonator mode is both damped and driven for all times. In such approaches feedback and control[35, 32], based on homodyne measurement, can be utilised to enhance the results. It is possible that similar application of feedback could help for our approach. However, even without any enhancement over our present results, it should be noted that such high fidelity, but probabilistic entanglement—heralded through the measurement outcome—has good use in Quantum Information Processing. Given the recent progress with superconducting qubit experiments, initial investigations of such entangling approaches should soon be possible. In the longer term, probabilistic but heralded entanglement generation can be used[36, 37] as a basis for efficient quantum computation using the cluster state approach[38].

Acknowledgments

The work of D.A.R. was supported by a UK EPSRC fellowship, and C.E.A.J. was supported by UK HP/EPSRC case studentship. BLG would like to thank the hospitality of the CMS of TU Wien.

References

[1] D. P. DiVincenzo. Quantum Computation. *Science*, 270:255, 1995.

[2] Y. Nakamura, Yu. A. Pashkin and J. S. Tsai. Coherent control of macroscopic quantum states in a single-Cooper-pair box. *Nature*, 398:786, 1999.

[3] D. Vion, A. Aassime, A. Cottet, P. Joyez, H. Pothier, C. Urbina, D. Esteve and M. H. Devoret. Maniputating the quantum state of an electrical circuit. *Science*, 299:866, 2002.

[4] I. Chiorescu, Y. Nakamura, C. J. P. M Harmans, J. E. Mooij. Coherent quantum dynamics of a superconducting flux-qubit. *Science*, 299:1869, 2003.

[5] Y.A. Pashkin, T. Yamamoto, O. Astafiev, Y. Nakamura, D.V. Averin and J.S. Tsai. Quantum oscillations in two coupled charge qubits. *Nature*, 421:823, 2003.

[6] A.J. Berkley, H. Xu, R. C. Ramos, M. A. Gubrud, F. W. Strauch, P. R. Johnson, J. R. Anderson, A. J. Dragt, C. J. Lobb and F. C. Wellstood. Entangled macroscopic quantum states in two superconducting qubits. *Science*, 300:1548, 2003.

[7] R. McDermott, R. W. Simmonds, M. Steffen, K. B. Cooper, K. Ciak, K.D. Osborn, S. Oh, D.P. Pappas and J.M. Martinis. Simultaneous state measurement of coupled josephson phase qubits. *Science*, 307:1299, 2005.

[8] A. J. Leggett. Testing the limits of quantum mechanics: motivation, state of play, prospects. *J. Phys. Condens. Matter*, 14:R415, 2002.

[9] A. J. Leggett. How far do epr-bell experiments constrain physical collapse theories? *J. Phys. A*, 40:3141, 2007.

[10] T. Yamamoto, Y.A. Pashkin, O. Astafiev, Y. Nakamura and J.S Tsai. Demonstration of conditional gate operation using superconducitng charge qubits. *Nature*, 425:941, 2003.

[11] M. Steffen, M. Ansmann, R. C. Bialczak, N. Katz, E. Lucero, R. McDermott, M. Neeley, E. M. Weig, A. N. Cleland, J. M. Martinis. Measurement of the entanglement of two superconducting qubits via state tomography. *Science*, 313:1423, 2006.

[12] A. Wallraff, D. I. Schuster, A. Blais, L. Frunzio, R.- S. Huang, J. Majer, S. Kumar, S. M. Girvin and R. J. Schoelkopf. Strong coupling of a single photon to a superconducting qubit using circuit quantum electrodynamics. *Nature*, 431:162, 2004.

[13] A. Wallraff, D. I. Schuster, A. Blais, L. Frunzio, J. Majer, S. M. Girvin, R. J. Schoelkopf. Approaching unit visibility for control of a superconducting qubit with dispersive readout. *Phys. Rev. Lett.*, 95:060501, 2005.

[14] D. I. Schuster, A. A. Houck, J. A. Schreier, A. Wallraff, J. M. Gambetta, A. Blais, L. Frunzio, B. Johnson, M. H. Devoret, S. M. Girvin and R. J. Schoelkopf. Resolving photon number states in a superconducting circuit. *Nature*, 445:515, 2007.

[15] I. Chiorescu, P. Bertet, K. Semba, Y. Nakamura, C. J. P. M Harmans and J. E. Mooij. Coherent dynamics of a flux qubit coupled to a harmonic oscillator. *Nature*, 431:159, 2004.

[16] J. S. Bell. On the einstein podolsky rosen paradox. *Physics*, 1:195, 1964.

[17] J. E. Marchese, M. Cirillo and N. Grnbech-Jensen. Classical analysis of phase-locking transients and rabi-type oscillations in microwave-driven josephson junctions. *Phys. Rev. B.*, 73:174507, 2006.

[18] A. Lupascu, E. F. C. Driessen, L. Roschier, C. J. P. M. Harmans, J. E. Mooij. High-contrast dispersive readout of a superconducting flux qubit using a nonlinear resonator. *Phys. Rev. Lett.*, 96:127003, 2006.

[19] E. Knill, R. Laflame and G.J. Milburn. A scheme for efficient quantum computation with linear optics. *Nature*, 409:46, 2001.

[20] T. Meunier, A. Le Diffon, C. Rueff, P. Degiovanni and J.-M. Raimond. Entanglement and decoherence of n atoms and a mesoscopic field in a cavity. *Phys. Rev. A*, 74:33802, 2006.

[21] B. W. Shore and P. L. Knight. Topical review: The Jaynes-Cummings model. *J. Mod. Opt*, 40:1195, 1993.

[22] J. Gea-Banacloche. Atom and field state evolution in the Jaynes-Cummings model for large initial fields. *Phys. Rev. A*, 44:5913, 1991.

[23] E. T. Jaynes and F. W. Cummings. Comparison of quantum and semiclassical radiation theories with application to the beam maser. *Proc IEEE*, 51:89, 1963.

[24] M. Tavis and F. W. Cummings. Exact solution for an n-molecule-radiation-field hamiltonian. *Phys. Rev*, 170:279, 1968.

[25] M. S. Iqbal, S. Mahmood M. S. K. Razmi and M. S. Zubairy. Interaction of two two-level atoms with a single-mode quantized field. *J. Opt. Soc. Am. B*, 5:1312, 1988.

[26] C. W. Gardiner and P. Zoller. *Quantum Noise*. Springer, Berlin, 1991.

[27] N. Imoto, H. A. Haus, and Y. Yamamoto. Quantum nondemolition measurement of the photon number via the optical kerr effect. *Phys. Rev. A*, 32:2287, 1985.

[28] G. J. Milburn and D. F. Walls. State reduction in quantum-counting non-demolition measurements. *Phys. Rev. A*, 30:56, 1984.

[29] T. Tyc and B. C. Sanders. Operational formulation of homodyne detection. *J. Phys. A*, 37:7341, 2004.

[30] A. Blais, J. Gambetta, A. Wallraff, D. I. Schuster, S. M. Girvin, M. H. Devoret and R. J. Schoelkopf. Quantum-information processing with circuit quantum electrodynamics. *Phys. Rev. A*, 75:032329, 2007.

[31] T. P. Spiller, K. Nemoto, S. L. Braunstein, W. J. Munro, P. van Loock, and G. J. Milburn. Quantum computation by communication. *New J. Phys.*, 8:30, 2006.

[32] M. Sarovar, H.-S. Goan, T. P. Spiller, and G. J. Milburn. High-fidelity measurement and quantum feedback control in circuit qed. *Phys. Rev. A.*, 72:062327, 2005.

[33] R. Ruskov and A. N. Korotkov. Entanglement of solid-state qubits by measurement. *Phys. Rev. B*, 67:241305(R), 2003.

[34] S. Schneider and G. J. Milburn. Entanglement in the steady state of a collective-angular-momentum (dicke) model. *Phys. Rev. A.*, 65:042107, 2002.

[35] J. Wang, H. M. Wiseman and G. J. Milburn. Dynamical creation of entanglement by homodyne-mediated feedback. *Phys. Rev. A.*, 71:042309, 2005.

[36] S. D. Barrett and P. Kok. Efficient high-fidelity quantum computation using matter qubits and linear optics. *Phys. Rev. A*, 71:060310(R), 2005.

[37] L.-M. Duan and R. Raussendorf. Efficient quantum computation with probabilistic quantum gates. *Phys. Rev.Lett.*, 95:080503, 2005.

[38] R. Raussendorf and H. J. Briegel. A one-way quantum computer. *Phys. Rev. Lett.*, 86:5188, 2001.